Catalysis Today 138 (2008) 216–221

Contents lists available at ScienceDirect

Catalysis Today

journal homepage: www.elsevier.com/locate/cattod

Negative apparent kinetic order in steady-state kinetics of the water-gas shift reaction over a Pt–CeO_2 catalyst

F.C. Meunier[a,b,*], G. Yablonsky[c,d,**], D. Reid[a], S.O. Shekhtman[a], C. Hardacre[a], R. Burch[a], M. Lazman[e]

[a] CenTACat, School of Chemistry and Chemical Engineering, Queen's University Belfast, Belfast BT9 5AG, Northern Ireland, UK
[b] Laboratoire de Catalyse et Spectrochimie, ENSICAEN, CNRS, University of Caen, 14050 Caen, France
[c] Saint Louis University, Parks College, St. Louis, MO 63103, USA
[d] Washington University, Department of Chemical Engineering, St. Louis, MO 63130, USA
[e] Aspen Technology, Calgary, Alberta, Canada T2P 1H5

ARTICLE INFO

Article history:
Available online 7 July 2008

Keywords:
Hydrogen
CO
Water-gas shift
Platinum
Ceria
Kinetics

ABSTRACT

The kinetics of the water-gas shift reaction were studied on a 0.2% Pt/CeO_2 catalyst between 177 and 300 °C over a range of CO and steam pressures. A rate decrease with increasing partial pressure of CO was experimentally observed over this sample, confirming that a negative order in CO can occur under certain conditions at low temperatures. The apparent reaction order of CO measured at 197 °C was about −0.27. This value is significantly larger than that (i.e. −0.03) reported by Ribeiro and co-workers [A.A. Phatak, N. Koryabkina, S. Rai, J.L. Ratts, W. Ruettinger, R.J. Farrauto, G.E. Blau, W.N. Delgass, F.H. Ribeiro, Catal. Today 123 (2007) 224] at a similar temperature. A kinetic peculiarity was also evidenced, i.e. a maximum of the reaction rate as a function of the CO concentration or possibly a kinetic break, which is sometimes observed in the oxidation of simple molecules. These observations support the idea that competitive adsorption of CO and H_2O play an essential role in the reaction mechanism.

1. Introduction

The water-gas shift reaction (WGS, $CO + H_2O \rightarrow CO_2 + H_2$) is an industrially important reaction, the main applications of which include hydrogen production for ammonia synthesis and hydrotreating of petroleum stocks. This reaction found a recent wider application in reforming systems for the production of clean hydrogen for fuel cells [1,2]. The WGS has a dual purpose for fuel cells, firstly produce hydrogen, which acts as the fuel and, secondly, remove CO, which is a poison to the platinum anode of the fuel cell. The WGS is exothermic and therefore the highest reaction yields would be achieved at the lowest possible temperature, and reactors operating below 120 °C would offer substantial benefits. At such low temperatures the reaction is kinetically limited, and the current major research target is to develop efficient and durable low-temperature catalysts. Industrially used Cu-based materials present a high low-temperature activity, but are highly pyrophoric and more robust alternatives are needed. Ceria-supported noble metal catalysts are currently considered as potential candidates for achieving such targets [3–18].

The reaction mechanism of the water-gas shift reaction over noble metal-promoted ceria has been the subject of much debate over the past years. Similarly to the case of Cu and magnetite-based industrial catalysts [19–23], two main types of reaction mechanism have been proposed. First, a redox (i.e. regenerative) route has been suggested, in which CO adsorbs on a Pt site and is oxidised by oxygen atoms from the ceria with re-oxidation of the ceria occurring by reaction with H_2O [24,11,25,26]. A second non-redox mechanism, so-called associative mechanism, has also been proposed and several groups have suggested surface formate species as main reaction intermediate, mostly based on IR studies [12,27–29]. Lefferts and co-workers have also proposed a mechanism involving both formate as well as a redox cycle on the support [30]. However, recent quantitative work combining operando DRIFTS and isotopic labelling techniques has unambigu-

---

[*] Corresponding author at: Laboratoire Catalyse et Spectrochimie, CNRS-ENSICAEN, University of Caen, 6 Boulevard du Marechal Juin, 14050 Caen Cedex, France. Tel.: +33 231452731; fax: +33 231452822.

[**] Corresponding author at: Saint Louis University, Parks College, St. Louis, MO 63103, USA.

E-mail addresses: frederic.meunier@ensicaen.fr (F.C. Meunier), gy@seas.wustl.edu (G. Yablonsky).

0920-5861/$ – see front matter © 2008 Elsevier B.V. All rights reserved.
doi:10.1016/j.cattod.2008.05.023

ously shown that the formates that are seen by IR spectroscopy are not part of the main reaction pathway on Pt and Au catalysts supported on ceria, zirconia or $CeZrO_4$ [26,16,31]. Other surface species such as CO–OH adducts have also been proposed as a potential reaction intermediates in the case of an associative mechanism [32].

Surprisingly, there seems to have been relatively few detailed kinetic studies of the WGS over noble metal supported on ceria, despite the fact that apparent kinetic orders and apparent activation energies of steady-state kinetic dependencies often give clues to the reaction mechanism. Since the 1960s, more attention from researchers in kinetics was paid to non-trivial peculiarities of steady-state reaction rate dependencies (e.g. negative kinetic order, discontinuities or kinetic breaks, two-branch kinetic behaviour or multiplicity) in catalytic oxidations of simple molecules. Regarding the conversion of CO, especially in oxidation over metals and metal oxides, a CO negative order and kinetic breaks in the corresponding kinetic dependencies are well known peculiarities [33–35]. Kinetic “breaks” have also been detected in hydrogen oxidation over polycrystalline Pt systems [36–40]. Moreover, peculiarities such as “break” and “multiplicity” are considered to be one of the interesting features found in kinetics of heterogeneous catalysis, which can be used to reveal detailed mechanisms. Using rigorous mathematical analysis, it was demonstrated that these phenomena are kinetic fingerprints of some mechanisms, particularly for those that include competitive adsorption of reactants [33–35]. Combined with independent physico-chemical measurements, such kinetic information allowed understanding complex mechanisms and estimating their parameters. While many spectroscopic studies regarding the WGS over ceria-supported noble metal catalysts have been reported [41–43], relatively few detailed kinetic-based papers are currently available (Table 1).

Several studies reported zeroth order in CO. The physical meaning of a zeroth kinetic can be that the reactant adsorption rate constant is high, causing the saturation of the related adsorption sites. A first order for CO can sometimes be related to the fact that the surface coverage is directly proportional to CO-gas phase concentration (e.g. following Henry’s law) and this adsorbed species is then converted in the step determining the overall reaction rate. Jacobs et al. [47] carried out experiments on Pt/CeO_2 under high H_2O/CO ratio conditions. DRIFTS studies carried out at high temperatures revealed that the surface coverage of CO was low under these conditions, while the effective CO reaction order was +1.

To our knowledge, the work by Ribeiro and co-workers [48] is the only example in the literature reporting a (slightly) negative kinetic order with respect to CO of −0.03 over Pt/CeO_2. A negative order may indicate that CO adsorbs competitively with other reagents or intermediates. Grenoble et al. [44] reported a negative order for the WGS over 5% Ni, 2% Pt and 1% Ru supported on Al_2O_3. A bifunctional process was proposed: (1) CO associatively and water dissociatively adsorbed on the metal, while (2) water also adsorbed on the support forming a formic acid intermediate, which migrated to the metal and decomposed to CO_2 and H_2. Therefore, it was assumed that the negative kinetic order essentially arised from the competition between CO and water for the metal sites. This assumption is somewhat controversial in the case of Pt, which is not known to activate water.

Gorte et al. showed that the nature of the ceria-supported metal did not affect the WGS rate below 400 °C [11], suggesting that the rate-determining step was actually related to a step involving ceria. A bifunctional mechanism was proposed, in which CO adsorbed on the metal reacted with ceria lattice oxygen to form CO_2, with water subsequently reoxidising the support. Several authors have used microkinetic models to represent the water-gas shift activity. Wheeler et al. [50] derived a rate expression for non-supported noble metals, in which a negative CO order could be derived (although not measured experimentally):

$$r'' = \frac{k_f K_{CO} K_{H_2O} P_{CO} P_{H_2O} - k_b K_{CO_2} K_{H_2} P_{CO_2} P_{H_2}}{(1 + K_{CO} P_{CO})^2}$$

where k_f and k_b denotes the rate constant of the forward and backward reaction, respectively; the K and P terms are the adsorption equilibrium constants and gas partial pressures, respectively. According to this equation the CO order becomes −1 at high partial pressures of CO. Mhadeshwar and Vlachos [51], using a complex microkinetic model reduced to a one-step rate equation have also theorized a possible negative order for CO for Pt based catalysts. Callaghan et al. [52] and Ovesen et al. [53] have performed substantial microkinetic analysis on copper-based catalysts. An interesting feature in the work of Callaghan et al. [52] was that the model incorporates both a formate and redox mechanism at low temperatures and a modified redox mechanism at higher temperatures. While Ribeiro and co-workers [48] proposed six and seven-step redox mechanisms for the WGS over

Table 1

Selected literature data reporting kinetic studies of the WGS reaction over ceria-based catalysts

Catalyst	T (°C)	E_{act} (kJ/mol)	Reaction orders				Reference
			CO	H_2O	CO_2	H_2	
Base metals							
5% Ni/Al_2O_3	250	78.2	−0.14	0.62			[44]
8% CuO/CeO_2	240	56	0.9	0.4	−0.6	−0.6	[45]
5% CuO/Ce–La–O	175–300						[5]
In excess CO		30.4	0	1	–	–	
In excess water		19.2	1	0	–	–	
Noble metals							
CeO_2	300	60 ± 4	0.3	–	–	–	[11]
Rh/CeO_2		44 ± 4	0	1	–	–	
Pt/CeO_2		44 ± 4	0	1	–	–	
Pd/CeO_2 (low T calcination)		44 ± 4	0	–	–	–	
Pd/CeO_2 (high T calcination)		84 ± 4		–	–	–	
Pd/CeO_2	200	38	0	0.5	−1	−0.5	[46]
Pt/CeO_2			1	0 excess H_2O	–	–	[47]
Pt/CeO_2			−0.03	0.44	−0.1	−0.38	[48]
0.79% $Pt/CeO_2/Al_2O_3$	200–400	78	0.13	0.49	−0.12	−0.45	[49]

One $Ni–Al_2O_3$ sample is also reported.

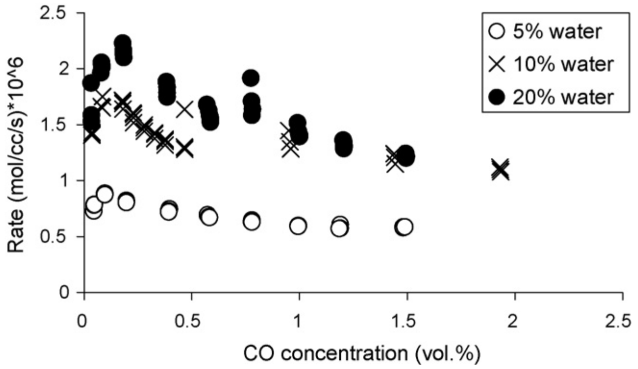

Fig. 1. Rate of CO conversion to CO_2 for various CO concentrations in the presence of 5%, 10% and 20% water. Temperature = 177 °C.

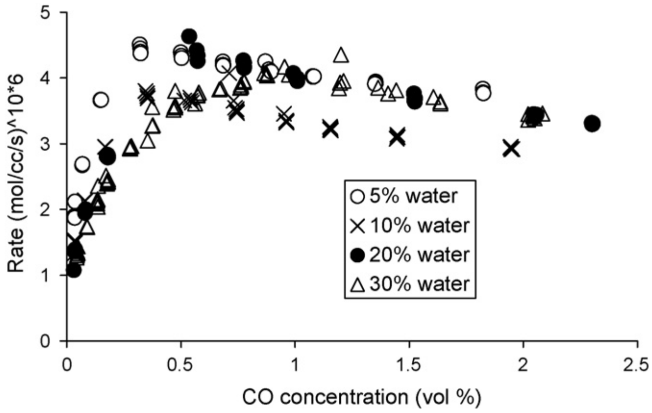

Fig. 3. Rate of CO conversion for various [CO] in 5%, 10% and 20% and 30% water during the WGS reaction. Temperature = 217 °C.

Pt/Al_2O_3 using a single type of sites (on the metal) that fitted the experimental data, these authors did not propose a model for the Pt/CeO_2 because of the increased difficulty of this (far more active) system.

In summary, there are few published data about the non-trivial kinetic peculiarities of the WGS reaction over different ceria-based catalysts; particularly regarding a negative kinetic order regarding CO and any kinetic discontinuity (i.e. break). In this paper, new experimental data on the WGS reaction using ceria-supported catalysts characterised by a negative CO order will be presented.

2. Experimental

The catalysts used this study was 0.2% Pt/CeO_2, supplied by Johnson Matthey. The BET surface area (measured with a Micromeritics ASAP 2010) for the 0.2% Pt/CeO_2 was 170 $m^2\,g^{-1}$ and the metal dispersion was 40%. The catalytic activity was measured using a 1/4 in. quartz plug flow reactor with quartz wool used to support the catalyst at both ends. The catalyst was subjected to a pre-treatment: reduction in pure H_2 from room temperature to 300 °C with a ramp rate of 10 °C/min. Typically 40 mg of the catalyst was used. Water was introduced by the saturation of a N_2 carrier gas and CO flowing through a distilled water saturator. The temperature of the water was controlled by a Grant thermostatic bath. The partial pressures of CO, H_2O and N_2, were controlled by Aera mass flow controllers. The concentration of the effluent gas from the reactor was determined using a PerkinElmer 5000 on-line gas chromatograph, equipped with a Chromosorb B column with a TCD and FID detector fitted with a methanizer to allow measurement of CO and CO_2.

Experimental data were obtained in the domain of both high and low conversions. Reaction isotherms were collected, by varying the CO partial pressure at a given partial pressure of water. Under high conversion in the domain of low CO concentration (less than 2%), the concentration profile within the reactor length was definitely non-uniform, and our reactor conditions should be characterised as the PFR-regime, and not CSTR. The apparent integral reaction rate was calculated using the following equation:

$$\text{Rate} = \frac{\text{Flowrate}^{\text{in}}}{\text{catalyst volume}}[C^{\text{out}}_{CO_2}]$$

In Figs. 1–5 the units were expressed as mol $cm^{-3}\,s^{-1}$

$$\text{Rate} = \frac{\text{Flow rate}}{\text{catalyst volume} \times 60} \times \frac{[C^{\text{out}}_{CO_2}]}{100 \times 22.4 \times 10^3} \times 10^6$$

in which the flowrate was expressed in mL min^{-1} and the catalyst volume in mL.

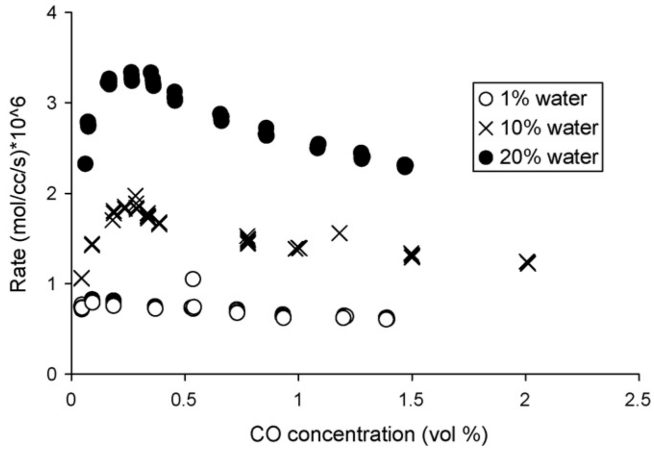

Fig. 2. Rate of CO conversion for various [CO] in 1%, 10% and 20% water during the WGS reaction. Temperature = 197 °C.

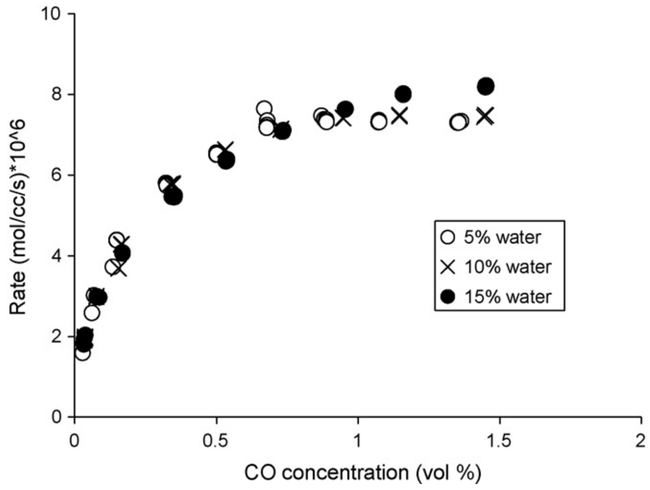

Fig. 4. Rate of CO conversion for various [CO] in 5%, 10% and 15% water during the WGS reaction. Temperature = 247 °C.

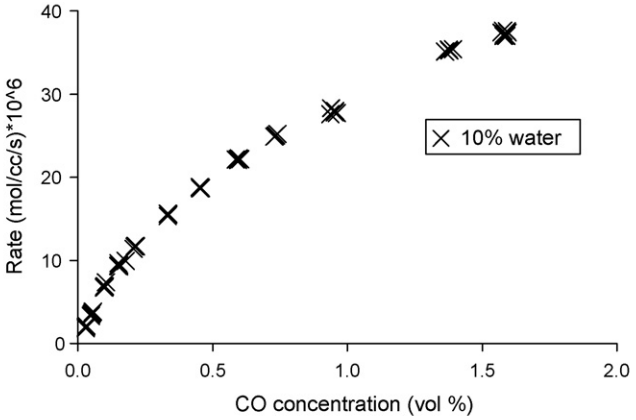

Fig. 5. Rate of CO conversion for various [CO] in 10% water during the WGS reaction. Temperature = 300 °C.

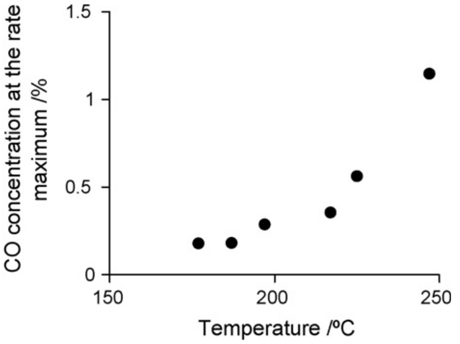

Fig. 6. Value of the CO concentration at the point of maximum rate as a function of temperature during the WGS reaction under 10% water.

3. Results and discussion

The CO molar concentration was varied between 0% and 2%, corresponding to partial pressures between 0 and ca. 2 kPa as we operated at ambient pressure (pressure and concentration are used throughout the text as equivalent terms). Various water concentrations were used, e.g. 1%, 5%, 10%, 20% and 30%. The temperature was changed in the interval 170–300 °C. The data presented in Figs. 1–5 are summarized in Table 2, which give the CO concentration and the rate of reaction at the rate maximum.

3.1. Influence of the temperature

Two temperature domains are clearly distinguishable. Firstly, a low temperature domain (177–217 °C, Figs. 1–3) is observed, characterised by a two-branch rate dependency located on each side of a rate maximum. CO positive and negative kinetic orders are observed at lower and higher concentrations, respectively. This phenomenon becomes more obvious at lower temperatures. Secondly, a high temperature domain is observed ($\geq$243 °C, Figs. 4 and 5), in which only a single branch with a positive CO order is observed over the experimental range investigated. At the boundary between these domains (observed at 217 °C) the rate maximum is very broad.

Table 2
Rate maximum characteristics derived from Figs. 1–5 and others not shown

Temperature (°C)	Water feed concentration (%)	CO concentration at the rate maximum (vol.%)	Rate maximum (10^{-6} mol cm^{-3} s^{-1})
177	5	0.094	0.876
	10	0.179	1.690
	20	0.184	2.130
187	10	0.180	1.880
197	1	0.094	0.783
	10	0.286	1.821
	20	0.359	3.259
217	5	0.322	4.373
	10	0.354	3.722
	20	0.777	4.153
	30	0.972	4.050
225	10	0.560	5.800
247	5	0.887	7.316
	10	1.146	7.458
	20	1.453	8.191[a]
265	10	1.844[a]	16.11[b]
300	10	1.590[a]	37.01[b]

[a] No maximum was observed within the experimental range.
[b] Reaction rate at the maximum CO pressure investigated.

3.2. Influence of water concentration

In the high temperature domain that shows no peculiarities, the water concentration influence on the kinetic dependence is not significant (Fig. 4). However, in the low-temperature domain the influence of water is quite complex. Fig. 1 shows a plot of the rate against CO concentration at 177 °C for three different water concentrations. The reaction rate clearly increases with the water concentration in this case. The CO concentration at which the rate maximum occurs increases with increasing water concentration (see Table 2). The change of slope around the rate maximum is rather sharp for all water concentrations, and could possibly be indicating the presence of a kinetic break [33–35]. Fig. 2 shows experimental results under three concentrations of water at 197 °C. Once again, the trend is similar to that reported in Fig. 1. There is a clear maximum and a negative order is observed on the high CO concentration branch. The rate increases with the water concentration and the position of the rate maximum again shifts to higher concentrations with increasing temperatures.

Fig. 3 shows results obtained at 217 °C under 5%, 10%, 20% and 30% water. In this case the effect of water concentration on the reaction rate is more complex. On the low CO concentration branch, the reaction rate decreases when increasing the water concentration from 5% to 10%, but remains approximately constant with further rises. On the contrary, on the high CO concentration branch the reaction rate increases with the rise of water concentration from 10% to 20% and then remains approximately constant with further rises. The point of maximum rate can be considered as a milestone that distinguishes regions with a different influence of the water concentration on the reaction kinetics.

A quantitative analysis of the data reported in Table 2 indicates that the position in terms of CO concentration of the rate maximum increases monotonically with the temperature (see Fig. 6 for the data collected under 10% water). The experimental data presented in Figs. 1–3 for the temperatures 177, 197, 217 °C also show the qualitative tendency of a monotonic correlation between reactant concentrations (CO and H_2O) at the point of maximum rate (Fig. 7). The relationship

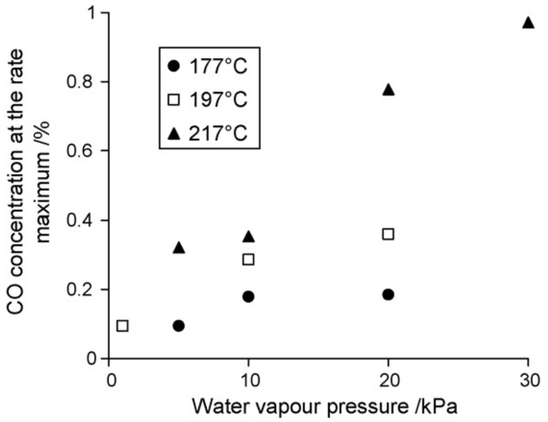

Fig. 7. Value of the CO concentration at the point of maximum rate as a function of water partial pressure (in kPa or vol.%) during the WGS reaction at various temperatures.

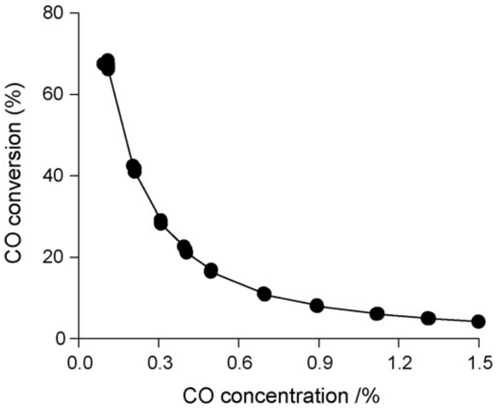

Fig. 9. CO conversion versus CO concentration data relating to the experiment carried out at 197 °C under 20% water.

between concentrations is likely a monotonic dependence of type:

$$[\mathrm{CO}] = \frac{K[\mathrm{H_2O}]}{1 + K[\mathrm{H_2O}]}$$

In some domains (5%, 10% at 177 °C; 5% 1%, 10%, 20% at 197 °C; 10%, 20%, 30% at 217 °C) this dependence can be considered as approximately linear, that is [CO] is proportional to [H_2O]:

$$[\mathrm{CO}] = K[\mathrm{H_2O}]$$

where the temperature dependence of the constant K is rather weak in the present case. It worth nothing that the negative CO reaction order is observed in the same parametric domain (i.e. low temperature) as that in which the influence of water concentration is also found.

In general, complex kinetic behaviour such as negative kinetic order, rate maximum and kinetic breaks can be caused by additional factors, first of all catalyst deactivation. For example a high ratio [CO]/[H_2O] may favour the formation of carbon lay down on the catalyst surface via the Boudouard reaction [54], and the subsequent deactivation and irreducibility of kinetic measurements. The reproducibility of the kinetic dependences was tested in the following experiment: the concentration of CO was increased up to 2 kPa and then decreased again (Fig. 8). The data points were perfectly reproducible within the experimental error, exhibiting no hysteresis. Therefore, catalyst deactivation was not the reason for the peculiarities (negative order and rate maximum) observed in this parametric domain. Clearly, this fact supports the idea that competitive adsorption of CO and H_2O play an essential role in the reaction mechanism.

3.3. Apparent reaction order

The calculation of the apparent reaction order with respect to CO requires using a set of data for which the CO conversion was low. Fig. 9 shows the CO conversion versus CO concentration for the experiment carried out at 197 °C under 20% water. The reaction order was calculated using the data points for which the conversion was lower than 12% (that is, $[\mathrm{CO}] > 0.6\%$), ensuring quasi-differential conditions. The logarithm of the dimensionless reaction rate versus that of CO concentration relating to the experiment carried out at 197 °C under 20% water is shown in Fig. 10. The apparent CO reaction order was ca. −0.27 in this case, that is much more negative than that reported by Ribeiro and co-workers at similar temperature and steam pressure [48]. The calculation of the reaction order in other cases will be reported elsewhere.

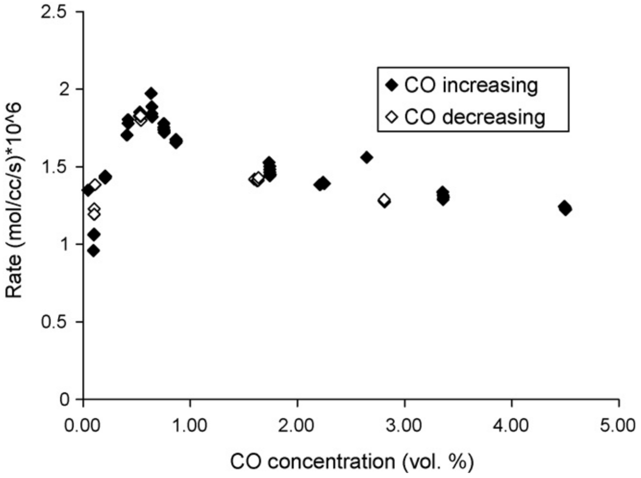

Fig. 8. Rate of CO conversion for various [CO] in 10% water during the WGS reaction. Temperature = 217 °C. The data points collected during the increase of [CO] are represented by the symbol ◆, while those recorded during [CO] decrease are represented by the corresponding open symbol (◇).

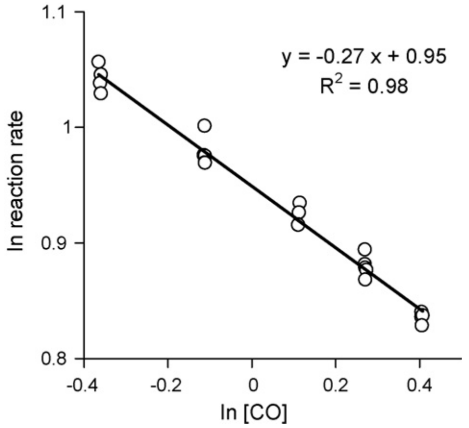

Fig. 10. Logarithm of the dimensionless reaction rate versus that of CO concentration relating to the experiment carried out at 197 °C under 20% water. The rates were calculated only using the data points for which differential conditions applied, i.e. CO conversion was less than 12%.

The maximum of the integral rate for the experiment carried out at 197 °C under 20% water (Fig. 2) occurred at a CO concentration of about 0.3%. The corresponding CO conversion was about 28% (Fig. 9), that is far from 100%, so the maximum in integral rate was not a calculation artefact, although we could not use these high conversion-data points to calculate a meaningful reaction order. These data qualitatively show that the apparent reaction order was positive in the low CO concentration region. The detailed analysis of the complete set of data and the derivation of the rate equations of various models will be described in a subsequent paper.

4. Conclusions

A kinetic study of the water-gas shift reaction on Pt/CeO_2 confirms that a negative order in CO can occur under certain conditions at low temperatures. The apparent reaction order of CO measured at 197 °C was about -0.27. This value is significantly larger than that reported by Ribeiro and co-workers (-0.03) at a similar temperature (200 °C). This observation supports the idea that competitive adsorption of CO and H_2O play an essential role in the reaction mechanism.

Acknowledgments

This work was supported by the European Social Funds and the EPRSC, under the CARMAC project. Janet Fisher from Johnson Matthey is also acknowledged for supplying the catalyst.

References

[1] A.F. Ghenciu, Curr. Opin. Solid State Mater. Sci. 6 (2002) 389.
[2] C. Song, Catal. Today 77 (2002) 17.
[3] A. Goguet, S.O. Shekhtman, R. Burch, C. Hardacre, F.C. Meunier, G.S. Yablonsky, J. Catal. 237 (2006) 102.
[4] B.I. Whittington, C.J. Jiang, D.L. Trimm, Catal. Today 26 (1995) 41.
[5] Y. Li, Q. Fu, M. Flytzani-Stephanopoulos, Appl. Catal. B 27 (2000) 179.
[6] J. Barbier Jr., D. Duprez, Appl. Catal. B 4 (1994) 105.
[7] Q. Fu, H. Saltsburg, M. Flytzani-Stephanopoulos, Science 301 (2003) 935.
[8] R.K. Hertz, J.A. Sell, J. Catal. 95 (1985) 166.
[9] T. Luo, R.J. Gorte, Catal. Lett. 85 (2003) 139.
[10] E.C. Su, W.G. Rothschild, J. Catal. 94 (1985) 166.
[11] T. Bunluesin, R.J. Gorte, G.W. Graham, Appl. Catal. B 15 (1998) 107.
[12] T. Shido, Y. Iwasawa, J. Catal. 141 (1993) 71.
[13] G. Jacobs, L. Williams, U. Graham, D. Sparks, B.H. Davis, J. Phys. Chem. B 107 (2003) 10398.
[14] A. Goguet, F.C. Meunier, D. Tibiletti, J.P. Breen, R. Burch, J. Phys. Chem. B 108 (2004) 20240.
[15] A. Goguet, R. Burch, Y. Chen, C. Hardacre, P. Hu, R.W. Joyner, F.C. Meunier, B.S. Mun, D. Thompsett, D. Tibiletti, J. Phys. Chem. C 111 (2007) 16927.
[16] F.C. Meunier, D. Reid, A. Goguet, S. Shekhtman, C. Hardacre, R. Burch, W. Deng, M. Flytzani-Stephanopoulos, J. Catal. 247 (2007) 277.
[17] A. Luengnaruemitchai, S. Osuwan, E. Gulari, Catal. Commun. 4 (2003) 215.
[18] G. Germani, P. Alphonse, M. Courty, Y. Schuurman, C. Mirodatos, Catal. Today 110 (2005) 114.
[19] C. Rhodes, G.J. Hutchings, A.M. Ward, Catal. Today 23 (1995) 43.
[20] G.C. Chinchen, M.S. Spencer, K.C. Waugh, D.A. Whan, J. Chem. Soc., Faraday Trans. 1 83 (1987) 2193.
[21] E.G.M. Kuijpers, R.B. Tjepkema, W.J.J. van der Wal, C.M.A.M. Mesters, S.F.G.M. Spronck, J.W. Geus, Appl. Catal. 25 (1986) 139.
[22] M. Tinkle, J.A. Dumesic, J. Catal. 103 (1987) 65.
[23] J.E. Kubsh, J.A. Dumesic, AIChE J. 28 (1982) 793.
[24] Q. Fu, A. Weber, M. Flytzani-Stephanopoulos, Catal. Lett. 77 (2001) 87.
[25] R.J. Gorte, Catal. Today 104 (2005) 18.
[26] D. Tibiletti, F.C. Meunier, A. Goguet, D. Reid, R. Burch, M. Boaro, M. Vicario, A. Trovarelli, J. Catal. 244 (2006) 183.
[27] G. Jacobs, B.H. Davis, Appl. Catal. A: Gen. 284 (2005) 31.
[28] A. Karpenko, R. Leppelt, V. Plzak, R.J. Behm, J. Catal. 252 (2007) 231.
[29] F.C. Meunier, D. Tibiletti, A. Goguet, S. Shekhtman, C. Hardacre, R. Burch, Catal. Today 126 (2007) 143.
[30] K.G. Azzam, I.V. Babich, K. Seshan, L. Lefferts, J. Catal. 251 (2007) 153.
[31] F.C. Meunier, A. Goguet, C. Hardacre, R. Burch, D. Thompsett, J. Catal. 252 (2007) 18.
[32] P. Liu, J.A. Rodriguez, J. Chem. Phys. 126 (2007) 164705.
[33] G.S. Yablonskii, V.I. Bykov, V.I. Elokin, A.N. Gorban, Kinetic models of catalytic reactions, in: R. Compton (Ed.), Comprehensive Chemical Kinetics, vol. 32, Elsevier Science Publishers, Amsterdam, 1991.
[34] M.Z. Lazman, G.S. Yablonskii, V.A. Sobyanin, Kinet. Katal. 27 (1) (1986) 67.
[35] G. Yablonsky, V.I. Elokin, Kinetic models of catalytic reactions, in: Perspective in Catalysis, Blackwell Science, 1992, pp. 199–250.
[36] V.L. Kuchaev, M.I. Temkin, Kinet. Katal. 13 (3) (1972) 3.
[37] V.L. Kuchaev, in: Soviet Union Seminar on Isotope Methods in Catalysis Mechanism Studies (in Russian), Novosibirsk, 1981, Preprint A2.
[38] H.M. Dannetun, D. Söderberg, I. Lundström, L.-G. Petersson, Surf. Sci. 152/153 (1985) 559.
[39] L.-G. Petersson, H.M. Dannetun, I. Lundström, Surf. Sci. 161 (1985) 77.
[40] L.-G. Petersson, H.M. Dannetun, I. Lundström, Surf. Sci. 163 (1985) 273.
[41] G. Jacobs, E. Chenu, P.M. Patterson, L. Williams, D.E. Sparks, G. Thomas, B.H. Davis, Appl. Catal. A 258 (2004) 203.
[42] D. Tibiletti, Ph.D. Thesis, School of Chemistry and Chemical Engineering, Queen's University Belfast, 2005.
[43] D. Tibiletti, A. Goguet, F.C. Meunier, J.P. Breen, R. Burch, Chem. Commun. 14 (2004) 1636.
[44] D.C. Grenoble, M.M. Esradt, D.F. Ollis, J. Catal. 67 (1981) 90.
[45] N.A. Koryabkina, A.A. Phatak, W.F. Ruettinger, R.J. Farrauto, F.H. Ribeiro, J. Catal. 217 (2003) 233.
[46] S. Hilaire, X. Wang, T. Luo, R.J. Gorte, J. Wagner, Appl. Catal. A 215 (2001) 271.
[47] G. Jacobs, L. Williams, U. Graham, G.A. Thomas, D.E. Sparks, B.H. Davis, Appl. Catal. A 252 (2003) 107.
[48] A.A. Phatak, N. Koryabkina, S. Rai, J.L. Ratts, W. Ruettinger, R.J. Farrauto, G.E. Blau, W.N. Delgass, F.H. Ribeiro, Catal. Today 123 (2007) 224.
[49] G. Germani, Y. Shuurman, AIChE 52 (5) (2006) 1806.
[50] C. Wheeler, A. Jhalani, E.J. Klein, S. Tummala, L.D. Schmidt, J. Catal. 223 (2004) 191.
[51] A.B. Mhadeshwar, D.G. Vlachos, Catal. Today 105 (2005) 162.
[52] C. Callaghan, I. Fishtik, R. Datta, M. Carpenter, M. Chmielewski, A. Lugo, Surf. Sci. 541 (2003) 21.
[53] C.V. Ovesen, B.S. Clausen, B.S. Hammershoei, G. Steffensen, T. Askgaard, I. Chorkendorff, J.K. Norskov, P.B. Rasmussen, P. Stolze, P. Taylor, J. Catal. 158 (1996) 170.
[54] A. Goguet, F.C. Meunier, J.P. Breen, R. Burch, M.I. Petch, A. Faur Ghenciu, J. Catal. 226 (2004) 382.